Scanning Microscopy

Volume 2 | Number 2 Article 9

1-29-1988

The Surfaces of Titanate Minerals, Ceramics and Silicate Glasses: Surface Analytical and Electron Microscope Studies

Sverre Myhra
Griffith University

Roger St.C. Smart
Griffith University

Peter S. Turner
Griffith University

Scanning Microscopy, Vol. 2, No. 2, 1988 (Pages 715-734)
Scanning Microscopy International, Chicago (AMF O'Hare), IL 60666 USA

0891-7035/88$3.00+.00

THE SURFACES OF TITANATE MINERALS, CERAMICS AND SILICATE GLASSES: SURFACE ANALYTICAL AND ELECTRON MICROSCOPE STUDIES

Sverre Myhra, Roger St.C. Smart* and Peter S. Turner

School of Science, Griffith University, Nathan, Queensland 4111, Australia.

(Received for publication February 23, 1987, and in revised form January 29, 1988)

Abstract

The review evaluates evidence of aqueous surface attack on glasses, titanate minerals and synthetic rock material (Synroc C) available from:- leach rates; surface analysis (XPS, SAM, SIMS); IR spectroscopy; and electron microscopy. Direct observations are described showing the formation of:- ion-exchanged, cation deficient layers; altered glass network and crystalline lattice layers and recrystallised, reprecipitated and surface-segregated layers. The titanate minerals react in the order perovskites > hollandite > fluorite structures (zirconolite, zirkelite, pyrochlore, polymignyte) > rutile. The formation of amorphous Ti-O films, recrystallising to TiO_2 (anatase and brookite), is observed on perovskite and hollandite surfaces. The surface reactivity of the titanate minerals is essentially the same in the ceramic assemblage Synroc C but additional microstructure (intergranular films, pores, triple points, minor phases) complicates the interpretation of first-day leach rates and depth profiles of leached discs. Reinterpretation of apparently congruent and incongruent dissolution data, using this evidence, is given for the glasses and titanate minerals. It is shown that solution analyses do not adequately describe the processes occurring in leaching and dissolution. The three major mechanisms of surface attack - ion-exchange, base catalysed hydrolysis of the network or lattice, and recrystallisation - are compared. Cation-exchange is very fast but limited to a layer no more than 20nm ahead of the reacted layer. Reaction of the titanate lattice is relatively slow and, in ceramics, appears to be limited by the grain size of the perovskite phase. *In situ* recrystallisation of amorphous TiO_x films to TiO_2 is fast above 100°C giving a polycrystalline discontinuous layer of varying depth (up to the grain size).

Keywords: titanates: minerals; surface analysis leaching; glasses; Synroc; electron microscopy; ceramics.

*Address for correspondence:
S.A. Surface Tech. Ctr., Sch. Chem. Technology, South Australia Inst. of Technology, P. O. Box 1, Ingle Farm, SA 5098, Australia
Phone No. (61)-8-343 3353.

Introduction

The reactivity of the surfaces of rock-forming minerals, as represented in leaching, dissolution and weathering reactions, is central to many important geological processes like soil formation, sedimentation and establishment of ground water compositions. The surface properties of silicate, alumino-silicate, and aluminate minerals have been quite extensively studied using the relatively new, surface specific techniques of X-ray photoelectron spectroscopy (i.e., XPS), scanning Auger microscopy /spectroscopy (i.e., SAM) and secondary ion mass spectrometry (i.e., SIMS) (e.g., Bancroft *et al*, 1979; Dillard and Koppelman, 1975; Koppelman, 1980). In contrast, the less common and more durable titanate minerals have received very little attention in studies designed to define the nature and extent of reaction at their surfaces under atmospheric and hydrothermal conditions of attack.

The challenge of providing safe disposal of high-level nuclear waste (HLW) for periods in excess of one million years has added a new dimension and considerable urgency to this area of study. There is a reasonable degree of concensus that secure disposal of HLW is best achieved using the multi-barrier principle (Hollister *et al.*, 1981). The first barrier is the immobilisation solid produced by the solidification of the liquid waste as part of a matrix that is physically and chemically highly resistant to change under conditions of self irradiation, high pressure, temperature and the presence of ground water. The second barrier may be a corrosion-resistant canister surrounding the HLW solid and designed to last at least 500 years in the final repository. The remaining barriers constitute a geological "package" to include a stable, inaccessible repository with minimal groundwater flow, reactivity with the solid "package" and thermal stress processes as well as engineered back-fill and sealing of the repository.

The present method of HLW disposal used by the nuclear power industry incorporates the waste into borosilicate glass. The glass matrix is amorphous and its flexible bonding

structure gives it a high tolerance, via self-annealing, for radiation-induced disorder. Glasses however, have several disadvantages for HLW incorporation. It is difficult to maintain homogeneity during preparation. Devitrification (i.e., crystallisation) can occur down the center-line of the canister and in localised, high-temperature regions of the solid (Jacquet-Francillon *et al*, 1982; Rusin *et al*, 1982). Devitrification can also occur due to self-irradiation and temperature rise. The stability of HLW glasses under hydrothermal repository conditions has been questioned (McCarthy *et al*, 1978; Myhra *et al*, 1984a). A maximum waste load capacity of 10 wt% has been recommended for these reasons but this loading is being exceeded in present fabrication processes.

Considerable progress has been made in the development of alternative, possibly second-generation, crystalline HLW solids. The hydrothermal stability of several of these solid forms exceeds that of the glasses and they can generally accept higher waste loadings without recrystallisation or degradation of leach resistance. Three types of solid have been developed that meet these criteria. A glass-ceramic, the crystalline phase of which is the mineral sphene ($CaTiSiO_5$) (Metson *et al*, 1982); an alumina-based waste form comprising several aluminate phases (Morgan *et al*, 1981); and Synroc, a titanate ceramic assemblage of several naturally occurring minerals (Ringwood *et al*., 1981). Our research group has undertaken Australian Government-sponsored scientific and technical evaluation of the Synroc waste form (e g. Segall *et al*, 1985; White et al, 1985; Cooper *et al*, 1985, 1986). The definition of the surface properties of the titanate minerals separately and in combination in the ceramic has been a major study in this research. The first objective of this review is to present a summary of the existing level of understanding of surface reactivity of titanate minerals.

The reactivity of mineral surfaces to aqueous attack in leaching and dissolution studies is often measured as elemental and mass loss rates to solution, expressed as g m^{-2} d^{-1}. In this rate expression, in addition to factoring out differences in surface area, it is usual (Lewis *et al*, 1982; Mendel, 1982) to ratio the amount of a particular element appearing in solution to the total amount in the bulk sample. This has the effect of suggesting that, if the rates of all elements are identical, they are dissolving in strict proportion to their composition in the surface. This is called "congruent" dissolution and is taken to imply that the constituents of a phase, and/or of all phases in a multi-phase ceramic, are dissolving uniformly as in a layer- by-layer process. "Incongruent" dissolution, on the other hand, is represented by different rates for different elements and is taken to imply preferential dissolution of some constituents of a phase, or of one phase over another in a multi-phase material. A single-phase solid is expected to show a depleted region in the solid surface if incongruent dissolution is observed by solution analysis. The surface techniques of XPS, SAM, SIMS and SEM allow us to examine the validity of this interpretation of leaching and dissolution behaviour. The nature of surface attack can be observed both chemically and structurally. The second objective of this review is to examine different cases of apparently incongruent dissolution in glasses, minerals and ceramics. It will be shown that the reality of surface alteration in these materials is not adequately represented by solution analyses.

The third objective of the review is to describe the three processes primarily responsible for alteration of titanate surfaces, namely ion exchange, base-catalysed hydrolysis of the titanate lattice, and recrystallisation. We will present some direct evidence for each process and discuss the contribution made by each process to the overall attack.

Materials and Methods

Materials

The borosilicate glasses described in this review have compositions as specified in Table 1. Glass #1 was poured to this composition by ACI, Australia. Glass #2 was prepared by Penberthy, Electromelt, Washington State, USA. Final compositions were verified by independent analysis at the Australian Atomic Energy Commission and by Lewis (1983).

The titanate minerals, perovskite ($CaTiO_3$), zirconolite and hollandite were made at Australian Atomic Energy Commission laboratories by cold pressing and sintering the raw oxides at temperatures of 1280-1400°C for 2-16h. Perovskites ($CaTiO_3$ and $BaTiO_3$) supplied by Anzon Limited (Newcastle, U.K.) were also used in some experiments. Full details can be found in Kesson *et al*. (1983) and Myhra *et al* (1983a). The minerals were characterised by SEM/EDS and XRD. They were all found to contain significant porosity; zirconolite has a minor phase of perovskite; and there is a trace of alumina in the hollandite phase.

Synroc B and C are made by the Sandia process (Dosch and Lynch, 1980; Levins *et al*., 1986) involving the hydrolysis of titanium tetra-isopropoxide and zirconium tetra-n-butoxide in the presence of NaOH to yield a powder that acts as a cation exchanger for Aℓ, Ba and Ca from nitrate solution. Simulated HLW (Table 2) is added as a nitrate solution to this precursor material in a subsequent step. The slurry is dried and calcined under a 3.5% H_2/N_2 reducing atmosphere at 750°C. It is finally hot-pressed at 1150°C with 2 wt% added Ti metal to control the redox potential.

Table 1

Nominal compositions (wt %) of elements in HLW glasses (at.% values in brackets)

	Glass #1	Glass #2*
B	4.2 (5.7)	2.9 (4.2)
O	39.2 (57.2)	41.1 (59.0)
Na	2.6 (3.9)	9.6 (10.8)
Mg	1.1 (1.6)	--
Si	15.6 (13.5)	18.6 (17.0)
P	--	0.2 (0.1)
K	4.1 (2.6)	
Ca	1.3 (1.2)	1.4 (1.4)
Ti	--	1.8 (1.0)
Cr	--	0.3 (0.1)
Fe	0.8 (0.2)	7.3 (2.0)
Ni	0.2 (0.1)	0.2 (0.1)
Zn	20.9 (11.7)	4.0 (2.4)
Rb	--	0.1 (<0.05)
Sr	2.1 (0.9)	0.3 (0.2)
Y	--	0.2 (<0.05)
Zr	1.1 (0.3)	1.4 (0.4)
Mo	1.3 (0.2)	1.6 (0.3)
Cs	--	1.0 (0.2)
Ba	1.6 (0.4)	0.4 (0.1)
La	--	0.5 (0.1)
Ce	0.8 (0.1)	1.3 (0.2)
Pr	--	0.6 (<0.05)
Nd	2.5 (0.3)	4.7 (0.4)
Sm	--	0.4 (<0.05)
Eu	0.2 (<0.05)	0.1 (<0.05)
U	0.5 (0.1)	--
	100.0	100.0

* This glass composition is the standard HLW glass PNL 76-68 specified by Pacific North West Laboratories (Lewis, 1983; Mendel, 1982)

Table 2

Typical composition (wt% oxide) of simulated waste for 20 wt% HLW Synroc C. From White *et al.* (1985).

Fission Products			Actinoids		
Rb_2O}			NpO_2}		
Cs_2O}	as Cs_2O	8.0	U_3O_8}	as UO_2	5.4
SrO }		2.6	PuO_2}		
BaO		3.8	Am_2O_3}	as Gd_2O_3	0.5
Y_2O_3		1.5	Cm_2O_3}		
La_2O_3}					
Ce_2O_3}	as Ce_2O_3	11.3			
Pr_6O_{11}}			Processing Contaminants		
Nd_2O_3 }	as Nd_2O_3	15.0			
Pm_2O_3 }			Fe_2O_3		3.7
Sm_2O_3		2.3	Cr_2O_3		0.8
Eu_2O_3 }	as Gd_2O_3	0.8	NiO		0.3
Gd_2O_3 }			P_2O_5		1.6
ZrO_2		12.1			
MoO_2		12.7			
TeO_2		1.8			
Tc_2O_7}					
RuO_2 }					
Rh_2O_3}	as Ag_2O	15.8			
PdO }					
Ag_2O }					
CdO }					

Methods

All leaching and dissolution studies described here were carried out in doubly distilled, deionised water (DDDW). Other studies on silica saturated water, ground water compositions and brine have been completed. We will limit our discussion to DDDW-leaching although it will be clear that other reactions and precipitation products will occur in these systems.

Results from a considerable variety of methods and techniques are reviewed. There are many important preparation conditions for samples, as polished discs, powders or ion beam-thinned TEM specimens, as well as details of instrumental conditions for reproducing results described here. There are also qualifications on results and conditions to be avoided in sample preparation (e.g., cutting and polishing discs in water). A full reproduction of this technical detail is not practicable within the scope of this short review.

Descriptions of all relevant preparation of samples and technical information on the application of the different methods and techniques can be found in:-

*leaching and dissolution studies of glasses (Lewis *et al.*, 1982; Lewis, 1983), titanate minerals (Kesson *et al.*, 1983; Myhra *et al.*, 1984b) and Synroc (Reeve *et al.*, 1983; Levins *et al.*, 1986; Segall *et al.*, 1985).

*XPS studies of glasses (Lewis *et al.*, 1982), titanate minerals (Myhra *et al.*, 1984b) and Synroc (Myhra *et al.*, 1983b).

*SIMS studies of glasses (Lewis 1983; Smart, 1985) and Synroc (Segall *et al.*, 1985; Smart, 1985).

*SAM studies of titanate minerals (Myhra *et al.*, 1984b) and Synroc (Myhra *et al.*, 1983b; Myhra *et al.*, 1984c).

*IR studies of glasses (Lewis *et al.*, 1982).

*SEM studies of glasses (Lewis, 1983), titanate minerals (White *et al.*, 1985) and Synroc (Cooper *et al.*, 1985).

*TEM studies of glasses (Lewis *et al.*, 1982), titanate minerals (Kastrissios *et al.*, 1987), and Synroc (White *et al.*, 1985).

Evidence of Surface Attack on Minerals, Glasses and Ceramics:- Methods and Techniques:-

Before discussing the specific case of surface reactivity of titanate minerals it is useful to consider the main lines of evidence used in studies of surface alteration of other minerals, glasses and multi-phase ceramics. The point of this consideration is to compare

the validity of inferences drawn from this data. The limitations of the different methods and techniques can, in some cases, pre-determine the nature of the conclusions reached, as for instance, when comparing analyses using energy dispersive spectroscopy (i.e. EDS) taken from depths of the order of a micrometre with those from XPS taken from depths of the order of 20Å.

The major methods and techniques used in these studies are:

-leach rates obtained by elemental analysis of a leachant solution and by mass loss of the solid sample expressed as

$$R = (a/A).(W/S.t) \qquad (1)$$

where R = elemental rate (g m^{-2} d^{-1}); a = mass of element in solution; A = mass of element in initial bulk sample; W = mass of initial sample; S = surface area; and t = time(d). This method conveniently represents the relative loss rates of the different elements in the surface but it has the disadvantage that it does not measure material reprecipitating or adsorbing on the solid surface or the walls of the leaching vessel (Sill, 1982; Mendel, 1982). It clearly does not give any information on the chemical and structural rearrangement of the surface during loss of material to solution. The use of sophisticated computer models to predict precipitates and reaction pathways (Wolery, 1979; Myhra *et al.*, 1984b), based on the solution analyses, can offset this difficulty but direct observation of these reaction products is obviously still highly desirable.

-XPS can give information directly on the chemical states of elements in the surface (i.e. first 4-5 atomic layers) before and after solution attack. With ion sputtering it can be used to develop depth profiles for these elements over micrometre depths but chemical information from these profiles must be treated with caution because the ion beam, in our case Ar^+, can have a significant reducing effect. For instance, Myhra *et al* (1983a, 1984b) have shown that Ti^{3+} and Ti^{2+} are progressively formed at both unattacked and hydrothermally attacked surfaces of titanate minerals as a function of ion dose as exemplified in Table 3. Additionally, XPS gives an averaged composition effectively representing the whole surface of fine-grained multi phase ceramics. In most spectrometers, its lateral resolution is >2mm but, in recent instrumentation, this can be reduced to 150 μm.

-SAM can provide lateral resolution of surface elements down to 500Å and can be used in the same depth-profiling mode as XPS. It has the potential to resolve compositional changes, in the form of elemental maps, in individual phases of ceramics. SAM is of great value in identifying localised precipitates and recrystallised products on these surfaces. In practice it is often limited by surface charging in poor semiconductors and insulators, particularly when differential charging occurs between phases. This has the effect of shifting the Auger signal suggesting loss of the elemental species in that region.

-SIMS is surface sensitive at the monolayer level and finds its main application in identifying and profiling minor elements in surfaces. XPS and SAM give quantitative information on surface elements down to about 0.1 at.% so that elements in lower concentration must be studied with SIMS. There are major difficulties with quantitation in SIMS because the ion signals are affected by compositional and structural changes in the solid matrix. Static SIMS, however has been shown to be reliable for profiling of thin intergranular films in ceramics (Smart, 1985). Lateral resolution is normally limited to about 150 μm, although recent technology allows isotopic imaging at the sub-μm level.

Table 3

Valence state changes in the Ti(2p) XPS species from $BaA\ell_2Ti_6O_{16}$ as a function of ion dose. Adapted from Myhra *et al.* (1984b).

Ion Dose (μA.min cm^{-2})	% Contribution Ti^{4+}	Ti^{3+}	Ti^{2+}
0	100	0	0
10	78	22	0
100	42	41	17
1000	40	41	19

-analytical scanning and transmission electron microscopy (SEM and TEM) are used to examine compositional and structural changes. SEM images are generally better than those from SAM but definition of the composition via EDS in regions with lateral and depth dimensions <1 μm is complicated by averaging of the X-ray signal over depths >1μm. The characteristic bell-shaped emission volume includes contributions from neighbouring grains in the signal. Many mineral grains and surface alteration layers have dimensions <200nm. TEM is particularly useful for studying altered surface layers where phase changes have occurred or where contrast changes can indicate lattice strain due to ion-exchange. Ion-beam thinning of TEM specimens introduces changes in surface reactivity, as we will discuss below, but comparison with powder samples can help to resolve questions of validity of results from this technique. The use of selected area electron micro-diffraction to identify new, small particles in amorphous surface layers can provide the most unequivocal evidence for surface reaction.

-infrared (IR) spectroscopy using surface-specific techniques (e.g., attenuated total reflectance (ATR), reflection-absorption

spectroscopy (IRRAS)) can provide useful information on changes to the structure of the lattice, particularly in relation to hydrolysis reactions and phase changes. The data are averaged over the whole surface and relate to depths of roughly 1/4 wavelength of the absorption observed, i.e. to depths determined by the vibration examined, but normally >0.5μm.

Electron microprobe has also been used (Ringwood *et al.*, 1981) but the interpretation of results from this technique has been questioned (White *et al.*, 1985) when applied to ceramics, like Synroc C, where the grain size is <500nm.

There are other more specialised techniques, like solid-state NMR, proton induced X-ray emission etc., but their application to these systems has been very limited to date.

In the context of the three objectives of this review, we can make clear why the use of several techniques from the above list is essential to a complete understanding of surface reactivity, by considering some specific examples of the leaching of borosilicate glasses containing simulated HLW studied in this way (Lewis, 1983; Lewis *et al.*, 1982; Cousens *et al.*, 1982a,b). The data comes from an extensive study of the hydrothermal leaching of 10 glass compositions (using non-radioactive elements to simulate the HLW) as a function of temperature, HLW loading, time, pH, pressure, etc. Two examples are specified in Table 1, Glass #1 being a 10% HLW composition based on the Materials Characterisation Centre, Pacific N.W. Labs PNL 72-68 composition, and Glass #2 being the standard 33% HLW PNL 76-68 formulation.

A wide variety of elements is evidently present in these glasses. They can be loosely grouped (Paul, 1982) into:- the ion-exchangeable, readily-leached alkali metal cations (e.g., Na, K, Cs, Rb); the network-forming elements (e.g., Si, B, O, P, Zr, Ti); and the network-modifying elements (e.g., Zn, Ni, Fe, Mo). The alkaline earth elements (e.g., Mg, Ca, Sr, Ba) can behave either like the alkali metal cations or like the network modifiers. In order to see these differences in behaviour in more detail, we will consider some of the different information provided by the above methods and techniques.

Table 4

Some leach rates (g m^{-2} d^{-1}) for mass loss and some elemental losses from Glass #1 subjected to attack in DDDW at 170°C for 60h.

Mass	Na	Si	Mg	Zn
27	110	31	0.124	0.0085

Table 4 gives some examples of leach rates for representative elements from Glass #1 subjected to hydrothermal leaching at 170°C. Incongruent dissolution is clearly indicated with rapid loss of alkali ions and very slow rates for Zn and Mg loss. In all of the glasses studied, the overall mass loss rate is closely approximated by the Si loss rate. Base catalysed hydrolysis of the borosilicate network via:-

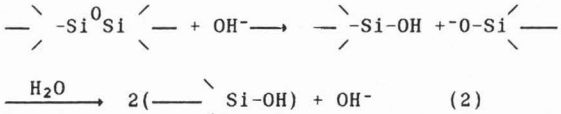

(2)

has been shown (Paul, 1982; Cousens *et al.*, 1982b) to be the reaction leading to breakdown and dissolution of the silicate groups. The leach rate data suggest that a surface layer should be found which is depleted in alkali ion (and Ca^{2+}, Ba^{2+}), hydrolysed to a siliceous, hydrogen-bonded structure, and containing increased concentrations of Zn, Mg, (as well as Fe, Ni, Ce, Nd).

Infrared spectroscopy using both ATR of the surface *in-situ* and transmission IR of the detached, altered surface, confirms the hydrolysed layer (Lewis, 1983), as illustrated in Fig. 1 for Glass #1. Initially (Fig. 1a), there is some absorption near 3500 cm^{-1} due to surface OH groups but this is entirely removed (Fig. 1b) by evacuation at 170°C. (The absorption near 2900 cm^{-1} is due to hydrocarbon contamination of the cell windows.) The ν(SiO) region of the spectra (i.e., 800-1600 cm^{-1}) is relatively featureless as is characteristic of amorphous silica mineral structures (Farmer, 1974). After aqueous leaching at 170°C for 60h, the surface layer shows strong, hydrogen-bonded ν(OH) absorption in the 3200-3500 cm^{-1} region and $\delta(H_2O)$ absorption near 1600 cm^{-1} (Fig. 1c). Evacuation at 170°C for 2h does not remove the ν(OH) absorption but $\delta(H_2O)$ is much reduced in intensity (Fig 1d). There is now evidence of silicate structure in the ν(SiO) region similar to spectra of crystalline minerals like olivine and talc (Farmer, 1974). A hydrated layer containing silicate groups is clearly indicated by these results.

This technique has been used to distinguish between glasses that form thick siliceous layers and those that do not (Hench *et al.*, 1980; Lewis, 1983) but the correlation with durability is not simple. Glasses with lower Si content generally form a substantially altered surface layer containing loosely bound water, because the network is weakened by the presence of the higher concentration of other ions, but, in some glasses, this layer can be stable and protective.

XPS can be used to generate depth profiles for representative elements in order to define the extent of the reacted layer. Fig. 2 shows profiles for Glass #1 before and after aqueous attack at 200°C for 1h. The concentrations are scaled to the bulk value which is taken to be

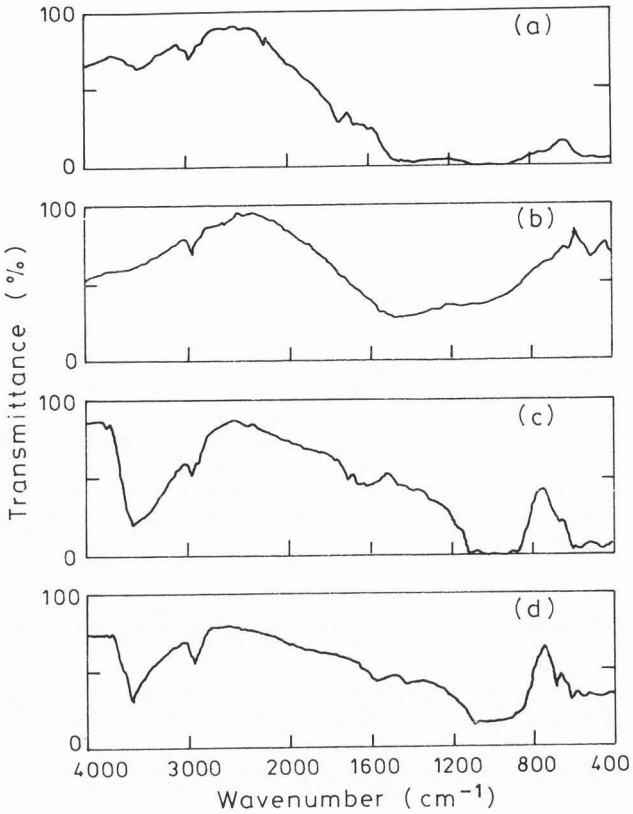

Fig. 1. Infrared spectra from surface layers of Glass #1, detached and prepared as 10wt% in KBr discs. a. initial surface. b initial surface after evacuation at 170°C for 1h. c. surface after hydrothermal attack in doubly distilled, deionised (DDD) water at 20°C for 18h (dried 200°C for 1h). d. after hydrothermal attack followed by evacuation at 170°C for 1h. (Redrawn from Lewis (1983)).

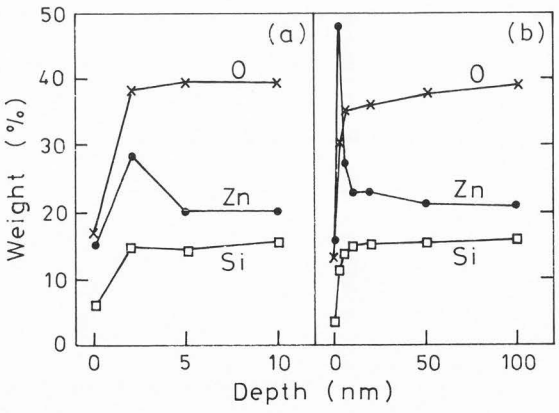

Fig 2. XPS depth profiles (~1nm min-¹) of O, Zn and Si in the surface of a polished disc of Glass #1 a. before and b. after hydrothermal attack in DDD water at 200°C for 1h, dried 200°C, 1h. Note change of depth scale from a. to b. (Reproduced from Lewis (1983)).

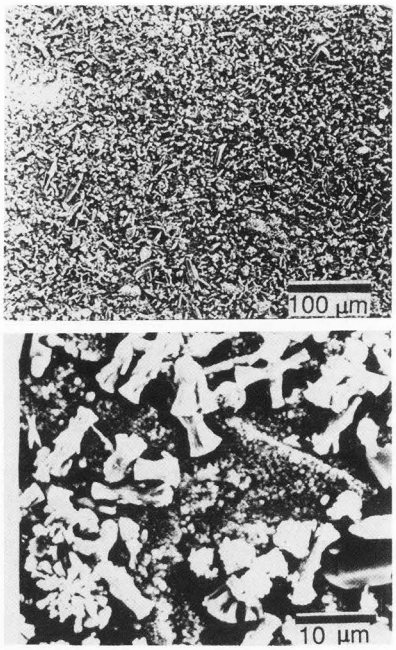

Fig. 3. SEM secondary electron images of the surface of a polished disc of Glass #1 after hydrothermal attack in DDD water at 170°C for 60h, dried 170°C, 1h. Bar is 100μm in 3a.; 10 μm in 3b. (Reproduced from Lewis (1983)).

the value at the end of the ion milling. The results illustrate the largely unchanged concentrations of Si and O in the hydrolysed siliceous layer. The striking feature however, is the accumulation of Zn within the first 10 nm of the surface. This observation is replicated in SIMS profiles of similar glass surfaces. The particular merit of the XPS and SIMS profiles is that they give a representation of the quite different composition profiles of different elements across the altered layer. Nevertheless, they do not tell the whole story as electron microscopy reveals.

SEM studies of the reacted surface show an almost uniform layer of material which is now conducting. Within this layer there are small crystallites of μm dimensions (Fig. 3) (Lewis, 1983), the concentration of which increases with the temperature and duration of hydrothermal reaction as well as the HLW loading. Different crystal forms appear also as the HLW loading is increased. TEM and electron diffraction were then used to characterise the structure of the altered layer. This showed that >90% of the layer is amorphous but that some specific crystalline phases form as localised precipitates within the hydrolysed region. For Glass #1, the mineral zinc hemimorphite, $Zn_4(OH)_2Si_2O_7.H_2O$, could be identified whilst a 25% HLW PNL 72-68 HLW glass showed zinc orthosilicate, Zn_2SiO_4 structure. It is equally interesting that, despite accumulation of Fe, Mg, Ni, Ce, and Nd at these surfaces, no crystalline forms incorporating these elements could be found.

Table 5

(a) Some leach rates (g m^{-2} d^{-1}) from Glass #2 in DDDW at 300°C for 1 day.

Mass	Si	Cs	Sr
120	70	110	0.23

(b) Leach rates (g m^{-2} d^{-1}) from Glass #2 in DDDW at 90°C for 7 days*

Mass	B	Ba	Ca	Cd	Cs	Fe
1.01	1.74	0.15	0.43	0.48	2.1	0.008

Mo	Na	P	Si	Sr	Ti	Zn
1.79	1.94	1.06	1.47	0.53	0.002	0.003

* Data from Mendel (1983).

Glass #2, with less Zn and more Fe in its formulation (Table 1), shows even more complex behaviour. Typical leach rates for some elements are given in Table 5, suggesting retention of Sr and Si and loss of the alkalis, e.g., Cs. SIMS profiles of the retained elements, recorded with progressive hydrothermal reaction, change markedly. A sequence in which fresh glass discs were reacted for 1,4 and 8 days at 150°C, and for 7 days at 300°C, in DDDW was examined. Fig. 4 illustrates SIMS profiles before and after hydrothermal attack for 7 days at 300°C in water. There are clear indications of precipitate formation, as sharp surface peaks, for Fe and Ti and more general surface enhancement of Zn and Si. The Fe profile, however, after reaction for 1 day at 150°C, shows a very broad peak covering 500 nm in which the bulk level is enhanced by a factor of 2.5. Increasing duration of reaction at 150°C, or reaction at 300°C, reduces this enhancement, until the remnants of it are seen as the broad peak near 400 nm as in Fig. 4. Zn is initially depleted by 50% over 100 nm during the first 8 days reaction at 150°C, but, after 7 days at 300°C, becomes slightly enhanced (180%) over 50 nm as in Fig 4. Ti is heavily depleted over 500 nm up to 8 days at 150°C but, at 300°C, develops the well-defined, near-surface enhancement of Fig.4. Si is slightly enhanced over 100 nm during the first 8 days at 150°C but is apparently depleted after 7 days at 300°C. (This may be due to changes in the Si^+ yield from the altered matrix in the reacted layer.) The profiles show B, Cs, Na heavily leached throughout these experiments. Transmission IR studies of the detached surface layer reveal

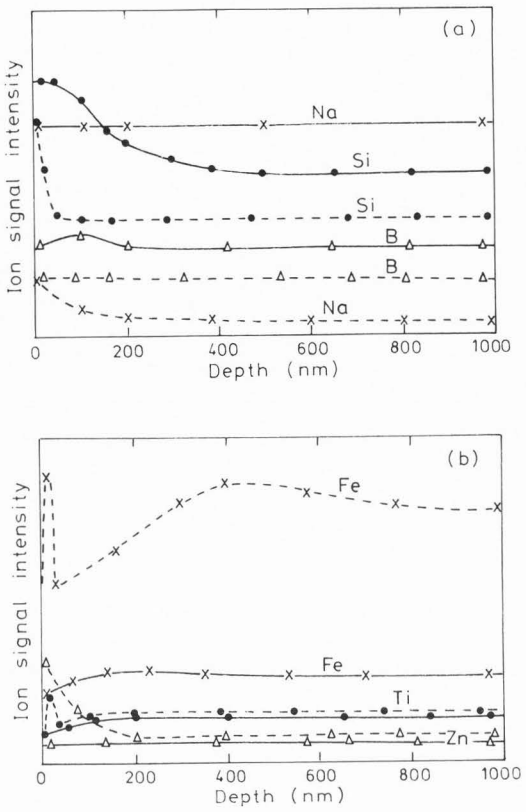

Fig. 4. SIMS profiles from the surface of a polished disc of Glass #2 before and after hydrothermal attack in DDDW water for 7 days at 300°C SIMS conditions:- 1kV Ar^+; 1.25 x 10^{-5} Acm^{-2}, charge compensated by low KE electron flood gun; 2x2 mm raster, 20% gated; etch rate (est.) ≈ 10 nm min^{-1}.
Full lines, unleached; broken lines, leached. a. x Na;● Si. ⊿ B; b. x Fe,● Ti, ⊿ Zn.

systematic formation of SiOH groups with increased attack and the loss of the ν(B-O) absorption near 1400 cm^{-1} even after one day reaction at 150°C. It is interesting that XRD shows no evidence of crystallinity in this reacted surface layer but TEM and electron microdiffraction find crystalline products as β-cristoballite and two pyroxene structures closely similar to wollastonite and rhodonite. Other studies (Buckwalter and Pederson, 1983; McVay and Buckwalter, 1984) have suggested that these crystalline products contain Fe and Zn. The crystalline proportion of the surface layer is certainly <5% in this case and it is evident that the particle size of this material is too small for XRD identification.

There is an extensive literature of other studies of glass leaching and dissolution using these techniques (e.g., Hench *et al.*, 1980; Clark and Hench, 1981; McCarthy *et al.*, 1980;

McVay and Pederson, 1981; Malm *et al.*, 1978; McIntyre *et al.*, 1980; Savage and Chapman, 1982). Our intention has been only to illustrate the type of information available and the main features of interpretation.

To summarise this section, it is evident that, in order to fully characterise surface reactivity of glasses, it is necessary to combine information from leach rates, surface analytical techniques and electron microscopy since each contributes an essential part of the overall description. This has been emphasised particularly by Clark and Hench (1981). We have also given evidence for three important processes in the reactivity of glass surfaces, namely ion exchange, base catalysed hydrolysis and reprecipitation of reaction products. We will see that these processes have parallels in the leaching and dissolution of crystalline minerals and ceramics.

The Surface Reactivity of Titanate Minerals

The titanate phases studied comprise those found in the Synroc C formulation, the Synroc form to be used for disposal of HLW from commercial power reactors (Ringwood *et al.*, 1981; Reeve *et al.*, 1983), plus some related phases. The principal phases in Synroc C have been identified as those listed in Table 6 (White *et al.*, 1985). Four distinct fluorite phases, zirconolite, zirkelite, pyrochlore and polymignyte, appear in sequence as the HLW loading is increased from 0 to 40 wt.%. They have the general formula $A_2B_2X_7$ where A,B = Ca, Zr, Ti, REE^{3+} (rare earth elements), Th^{4+}, U^{4+} and X = O. The simplest form, zirconolite as $CaZrTi_2O_7$ can be regarded as a layer structure in which planes of TiO_6 octahedra alternate with sheets of CaO_8/ZrO_7 polyhedra. Perovskite and its polytype are nominally $CaTiO_3$ as a nearly-cubic array of TiO_6 octahedra with Ca^{2+} Sr^{2+}, and REE^{3+} ions occupying the large interstice between the 8 octahedra. Synroc hollandite has the ideal formula $Ba(A\ell^{3+},Ti^{3+})_2Ti_6O_{16}$ and contains tunnels both one and two octahedra in width into which Ba^{2+}, Cs^+ and Rb^+ can substitute (with appropriate ordering to maintain charge balance). The structure of rutile has of course been much studied because of its ability to accommodate non-stoichiometry by the introduction of crystallographic shear planes. It can also accept a small amount of Zr replacing Ti but does not retain HLW elements. A complete review of these structures can be found in White *et al.*, (1985) and White and Fielding (1987).

A second perovskite, $BaTiO_3$, has also been studied with XPS and SAM.

The combination of the phases from Table 6 with some minor metal alloy phases in the"synthetic rock" ceramic Synroc C produces about 30 wt% fluorite phases, 30% hollandite, 15% perovskite, 15% rutile, <5% magnetoplumbite and β-alumina, and <5% alloy phases. The basic formulation, Synroc B, contains no HLW; Synroc C may have up to 40 wt% added HLW. A typical composition of Synroc C is given in Table 2,showing the additions of simulated fission products, actinoids and processing contaminants.

Table 6

Unit cell parameters for Synroc C phases. Adapted from White *et al.* (1985).

Phase Name/ Structure Type	System [a]	Cell Parameters a [Å]	b [Å]	c [Å]	α [°]	β [°]	γ [°]
Fluorite derivatives							
Zirconolite	m	12.611	7.311	11.444	90	100.52	90
Zirkelite[b]	tr	12.62	7.29	16.89	90	90	90
Pyrochlore[b]	c	12.61	7.26	17.84	90	90	90
Polymignyte[b]	o	2x12.37	7.28	17.41	90	90	90
Perovskite	o	5.37	7.64	5.44	90	90	90
Perovskite-Polytype	h	5.4	5.4	22.1	90	90	90
Rutile	te	4.58	4.58	2.95	90	90	90
Hollandite[c]	te	10.039	10.039	2.943	90	90	90
$BaTi_2Ti_6O_{16}$[d]	m	14.209	9.981	2.971	90	90	90
Magnetoplumbite (e.g. $CaA\ell_{12}O_{19}$)	h	5.576	5.576	21.97.	90	90	133.5
β-Alumina (e.g. $RbA\ell_{11}O_{17}$)	h	5.597	5.597	22.877	90	90	120
					90	90	120

[a] m: monoclinic, tr: trigonal, c: cubic, o: orthorhombic, h: hexagonal, te: tetragonal. [b] Non-standard C-centred cells. [c] Dimension of subcell axes. [d] Non-standard axial setting.

Although these individual titanate phases and their ceramic combination are obviously not natural minerals or rocks, they are based in their formulation on naturally occurring analogues known to have extremely high durability and tolerance to radioactive decay

processes (Ringwood, 1978). The structural modifications that are found with changes in HLW loading and composition provides a diversification of the system. They represent, therefore, a reasonable starting point for the characterisation of surface reactivity of other titanate minerals. We shall see that the mechanisms of attack are sufficiently general to give some confidence in their extrapolation to other systems. Elemental leach rates from hydrothermal (DDDW) reaction at 300°C over 14 days for the separate major phases are given in Table 7. They show that leaching is apparently incongruent in all cases with, again, alkali metal cations and Ca tending to leach faster and the lattice-forming Ti tending to be retained by the surface. Aℓ and Zr in hollandite and zirconolite respectively also seem to be retained by the surface.

Table 7

Leach rates (g m^{-2} d^{-1}) of titanate minerals as discs in DDDW at 300°C over 14 days (solution volume/surface area ratio 6.5 cm)

Perovskites			
$CaTiO_3$		$BaTiO_3$	
Ca	Ti	Ba	Ti
0.0138	<0.0002	0.033	<0.0003

Hollandite $BaAl_2Ti_6O_{16}$			Zirconolite $CaZrTi_2O_7$		
Ba	Aℓ	Ti	Ca	Zr	Ti
0.113	0.0066	<0.0008	0.0027	$<1.1\times10^{-5}$	<0.0002

We can now examine the evidence of depth profiles from XPS (Myhra *et al.*, 1983a, 1984b) to compare with the leach rate data. Fig. 5 shows a composition profile for zirconolite before (open symbols) and after (closed symbols) hydrothermal attack at 250°C for 14 days. (Zirconolite samples generally contain a minor phase of perovskite comprising <10 vol %). An ion dose (horizontal axis) of 1 μA.min from a 5kV Ar^+ beam at 20 μA.cm^{-2} is equivalent to removal of approximately 0.2nm of surface material. The profiles show that Ca is depleted by about 15% and Zr is enriched by about the same proportion to a depth of roughly 200nm. Oxygen and Ti are enriched and depleted, respectively, by <10% over the first 20nm only. This attack is relatively very severe. More moderate conditions with temperatures <150°C alter the elemental surface concentrations to very minor degrees normally involving <5% change. Given that the presence of the perovskite phase enhances the Ca leach rate, these observations are in accord with the leach rate data.

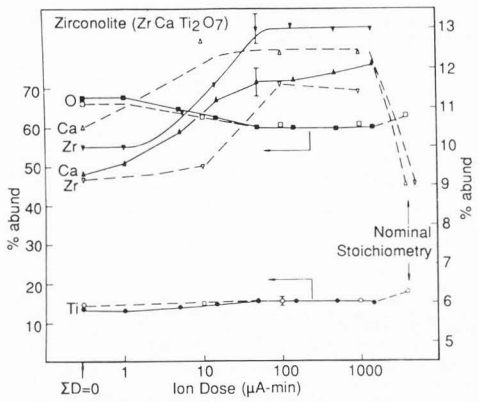

Fig. 5. XPS depth profiles (1 μA.min ≈ 0.2 nm) of zirconolite before (broken lines, open symbols) and after (full lines, filled symbols) hydrothermal attack at 350°C for 14 days. Nominal (bulk) stoichiometries are shown on right. Left hand scale (% abundance) is for Ti (o) O (□); r.h scale for Ca (△), Zr (▽). (Reprinted with permission from Myhra *et al.* (1984b)).

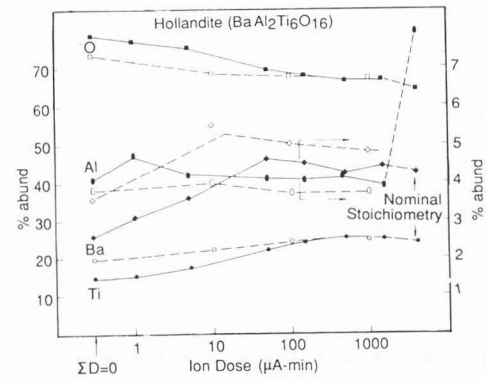

Fig 6. XPS depth profiles (1μA.min ≈ 0.2 nm) of hollandite before (broken lines) and after (full lines) hydrothermal attack at 350°C for 14 days. L.h. scale is for Ti (o) O ( ); r.h. scale is for Aℓ (O), Ba ( ). Typical error bars are as for Fig 5. Note discrepancy (in sensitivity factor) for Aℓ between measured and nominal bulk stoichiometry. (Reprinted with permission from Myhra *et al.* (1984b)).

Fig. 6 gives composition profiles for hollandite attack under the same conditions as those in Fig 5. Ba is substantially depleted by >25% over the first 200nm. Aℓ is slightly enhanced overall but, significantly, appears to show a region of particular enrichment near the surface. Ti and O behave as in zirconolite but the change in their respective abundances is larger suggesting more complete reaction of the titanate lattice over the first 20nm.

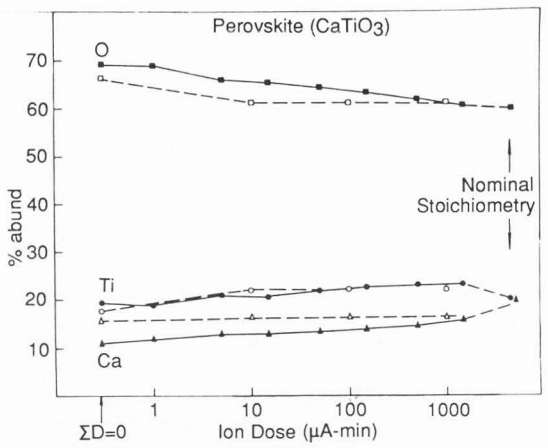

Fig. 7. XPS depth profiles (1μA.min $\approx$ 0.2 nm) of perovskite before (broken lines) and after (full lines) hydrothermal attack at 300°C for 19 days. Ti (o), O (□), Ca (Δ). Typical error bars are as for Fig. 5. (Reprinted with permission from Myhra *et al.* (1984b).

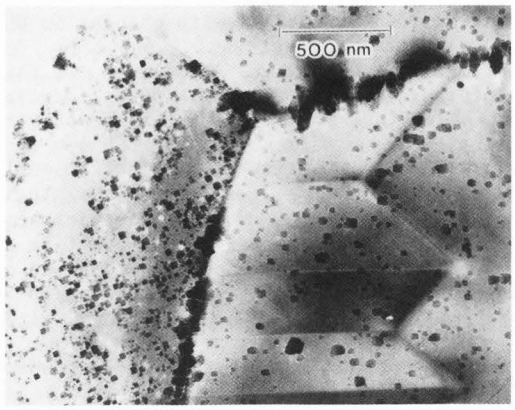

Fig 8. TEM micrograph of brookite and anatase crystallites on an Ar^+ ion beam-thinned disc of perovskite hydrothermally attacked for 4 days at 110°C. Note enhanced recrystallisation of TiO_2 along grain boundaries and on ℓ.h. perovskite grain.(Reprinted with permission from Kastrissios *et al.* (1987)).

Fig. 7 gives profiles for perovskite before and after hydrothermal attack at 300°C for 19 days. Ca is substantially depleted by >40% over 200nm but Ti does not appear to be as significantly affected as in the other two minerals. The behaviour of O is similar to that in the other two minerals.

$BaTiO_3$, after 12 days at 250°C, showed changes similar to those of Ca-perovskite, with Ba substantially depleted to 200nm, Ti not markedly affected and O enriched to about 20nm. The shapes and binding energies of the Ba and Zr (3d) XPS peaks were not identifiably altered in any way by hydrothermal attack of $BaTiO_3$, zirconolite or hollandite. The Ti(2p) envelopes of all phases generally showed an increase in the high binding energy Ti^{4+} component after leaching, with the leached $CaTiO_3$ and $BaTiO_3$ perovskites exhibiting high proportions of Ti^{4+} (e.g. 80%) than those for the other leached phases (eg., 67% for zirconolite). These changes might suggest the formation of (hydrated) TiO_2 on the surface. The Ca (2p) envelope from $CaTiO_3$ (but not zirconolite) develops a low binding energy component (~13%) corresponding to either a hydroxide or a carbonate species.

SAM examination (Myhra *et al.*, 1984b) of leached zirconolite (with minor perovskite phase) revealed a patchy, differentiated surface with particular areas that analysed as TiO_2, $CaCO_3$ and ZrO_2. A modified layer with bright secondary electron emission appears on both phases. For hollandite, bright secondary emission regions were also identified corresponding to $A\ell_2O_3$ (or AℓOOH) and some Ti- and Ba-rich areas, possibly TiO_2 and $BaCO_3$ respectively. This study was not fully developed because EM work proved to be more conclusive in the examination of altered surface products.

Analytical electron microscopy has added important information to the description of surface reactivity derived solely from leach rates and surface analysis. Perovskite, $CaTiO_3$, provides the simplest case. Fig. 8 is a TEM micrograph of an ion-beam thinned disc of perovskite subjected to hydrothermal reaction at 110°C for 4 days (Kastrissios *et al.*, 1987). Recrystallisation of TiO_2 is observed varying in concentration from particularly strong nucleation along grain boundaries to quite a low concentration as on the righthand crystal of Fig. 8. Careful electron microdiffraction study has shown that both brookite and anatase crystallites are formed, epitaxing with the (101) perovskite plane via the (011) brookite and {001} anatase planes. Perovskite, as a separate phase in zirconolite samples, is selectively lost and, after extensive high temperature leaching, is replaced as intergrown TiO_2 crystals formed in the surface "pores" left by the perovskite phase. SEM can also identify $CaCO_3$ among recrystallised products on the perovskite surface when the pH of the leachant rises above 9. In contrast, most of the Ca is in the solution if the pH is <5 during dissolution (Pham, unpublished report). The zirconolite surface in EM examination appears effectively unaltered even after high temperature attack for long periods (although it does collect some recrystallised TiO_2 adjacent to perovskite inclusions). The hollandite surface is attacked in a similar fashion to that of perovskite but to a less marked degree. TiO_2, $A\ell_2O_3$ (or AℓOOH) and either $BaCO_3$ or, if sulphate is present, $BaSO_4$ crystallites are observed. It is important to note that the titanate surfaces beneath these

crystalline products do not appear to form an extensive, hydrated layer similar to that found on glasses. In fact, they appear in SEM and TEM to be unaltered in contrast and morphology.

There have been a number of other studies of leaching of these phases (e.g., Ringwood *et al.*, 1981; Nesbitt *et al.*, 1981; Scheetz *et al.*, 1982; Freeborn and White, 1984; Kesson, 1983), the major parts of which agree with the description of the processes given here. There are, however,two discrepancies worthy of note. Ringwood *et al.*, 1981, using electron microprobe (i.e., ~1μm depth) analysis of hydrothermally reacted synthetic perovskite and weathered rims of natural perovskites, proposed a titania enriched "skin" on all three minerals after leaching and suggested that this film would be protective. We find that this TiO_2 layer is not continuous and that leaching of perovskite is essentially congruent (see next section). Nesbitt *et al* (1981) suggested, on thermodynamic grounds, that perovskite would react in silicate ground water as in:-

$$CaTiO_3 + SiO_2(aq) = CaTiSiO_5 \qquad (3)$$

to form sphene. We find only anatase and brookite on these surfaces under conditions of hydrothermal attack in silica saturated water (Myhra *et al.*, 1987). It appears that sphene itseIf is unstable under these conditions and also recrystallises to TiO_2 products.

Using the same techniques as those for the borosilicate glasses, we have not been able to observe infrared evidence for a persistent hydroxylated surface layer on these reacted titanate mineral surfaces. Both ν(OH) and $\delta(H_2O)$ absorptions are weak and are lost on evacuation at 100°C for 1h.

This review has used a small selection of data from a large body of work in each of these techniques collected over a six year study. To summarise the main conclusions resulting from the combination of these results on the individual titanate phases:

*the perovskites, $CaTiO_3$and $BaTiO_3$,leach relatively rapidly and <u>apparently</u> incongruently (see next section), selectively losing Ca and Ba to form recrystallised TiO_2 (as brookite and anatase) epitaxially on their surfaces. At high pH (only), reprecipitation of $CaCO_3$ and $BaCO_3$ also occurs. $BaSO_4$ is observed if sulphate is present in the solid or solution;

*zirconolite leaches relatively very slowly and nearly congruently (if due allowance is made for the minor perovskite phase). It does not appear to form extensive recrystallised products in short term. high temperature attack. There is some evidence of TiO_2 and ZrO_2-rich areas in SAM suggesting a kinetically limited formation of new phases in the longer term;

*hollandite is intermediate in properties with apparently incongruent selective leaching of Ba and retention of Aℓ (and Ti). It recrystallises to TiO_2, like perovskite but much more slowly and also forms an $A\ell_2O_3$ (or AℓOOH) product on its surface. Ba can again be observed in recrystallised form as $BaCO_3$ (at high pH) or $BaSO_4$;

*rutile is effectively unchanged by severe hydrothermal treatment on all evidence from these surface analytical and electron microscopic techniques.

We can now consider any changes introduced by combining these minerals into the synthetic ceramic assemblage, Synroc C (Table 6). In addition to possible synergistic effects between phases, there are new microstructural features like intergranular films, pores and glassy triple points, to be considered (Cooper *et al.*, 1986).

A typical set of leach rates for mass and some representative elements at 90°C for 0-1, 0-7 and 7-14 days, respectively, is given in Table 8. Elements which leach faster than the mass loss rate are Ba, Ca, Cs, Mo and Sr. Ti, Zr and Aℓ loss rates are much lower than the mass loss rate and are generally difficult to detect above the sensitivity limit for ICP analyses. From the individual mineral structures, it is expected that congruent leaching of Ba and Cs from hollandite should occur (similar tunnel sites) and this is roughly indicated in the data. Ca and Sr from perovskite (similar sites) should leach at the same rate but the additional concentration of Ca in zirconolite, which leaches very slowly, when incorporated into equation (1), tends to produce a slower rate for Ca than for Sr during the first 7 days of leaching. It is obvious that the rates for the leachable elements decrease very considerably after the first day, suggesting that a concentration gradient (or depletion zone) has been established in the solid.

<u>Table 8</u>

Leach rates (g m^{-2} d^{-1}) for a standard Synroc C (10% HLW) reacted in DDDW at 90°C for i) 0-1 day and ii) 0-7 days and iii) 7-14 days

	0-1 day	0-7 days	7-14 days
Mass	0.036	0.018	0.008
Aℓ	<0.0002	<0.0001	<0.0001
Ba	0.792	0.092	0.015
Ca	0.080	0.019	0.007
Cs	0.850	0.079	0.018
Mo	1.677	0.335	<0.031
Sr	0.192	0.026	<0.005
Ti	<0.001	<0.0001	<0.0001
Zr	<0.017	<0.0023	<0.0013

Other studies by Oversby and Ringwood (1982); Lewis *et al.*, (1982); Freeborn and White (1984), Sheetz *et al.*, (1982); Dosch *et et*, (1983) generally support these conclusions.

Quantitative XPS analyses of the surfaces (after 2.5nm has been removed by Ar^+ ion sputtering) of standard Synroc C samples before and after leaching (7 days at 150°C) gave the data in Table 9. The values for Mo, Cs (close to sensitivity limit) and Aℓ (insensitive and overlapped with Cs and Nd peaks) are unreliable but generally these results indicate that Ba,

Table 9

XPS atomic concentrations (%) from the surface of a standard Synroc C disc before and after leaching at 150°C for 7 days and from a fracture face

	Unleached Pol.face	Leached at 150°C	Fracture face	Fracture face, 20Å etch
Ti	18.5	19.5	14.2	16.8
O	70.9	65.4	60.4	61.3
Ca	3.8	3.7	2.9	3.0
Zr	1.3	1.9	0.8	1.0
Ba	0.8	0.6	0.9	1.0
Cs	0.1	<0.1	0.7	0.2
Aℓ*	4.4	8.7	19.7	16.7
Mo	0.2	0.1	0.2	0.1

* Inaccurate due to low sensitivity

Cs, Mo and Ca are leached whilst Ti, Zr and Aℓ are retained on the surface, in accordance with leach rate data. XPS profiles from Synroc C, before and after severe hydrothermal attack at 250-350°C, have been determined by Myhra *et al.*, (1984b) for the matrix elements Ca, O, Ti, Zr, Ba, Aℓ and for some observable HLW elements Fe, Sr, Mo, Cs, Ni. The profiles clearly show enhancement of Aℓ and Zr. Ti is depleted in these profiles as in the individual minerals (Figs 5-7), and Ba, Ca, Mo and Ni are also depleted in the surface. Fe is very substantially accumulated in the first 20nm. Values for Sr and Cs are considered unreliable but generally indicate Cs loss and Sr accumulation. (The Sr result does not agree with other data). The maximum depth of the modified layer, as for the separate minerals, is 200nm, and the changes in peak binding energies and shapes also agree with the individual mineral data. The Ti(2p), Zr(3d) and, particularly, the Aℓ(2p) peaks appear sharper after leaching, suggesting a narrower range of chemical states in the altered surfaces as would be found in recrystallised products.

The effect of other microstructural features on reactivity has been extensively examined (e.g. Cooper *et al.*, 1986; Clarke, 1981; Jantzen *et al.*, 1982). Fracture faces of the ceramic expose intergranular films which selectively accumulate Cs, Na, K, Aℓ (Table 9) and some Si impurity. Static SIMS profiles illustrate that these films are very thin (<20Å) as in Fig. 9, but can contain Cs and Na concentrations 3-5 times that of the bulk matrix. Both XPS and SIMS reveal (Cooper *et al.*, 1986) that Cs, Na and K are immediately lost by ion exchange to solution on exposure at room temperature. Pores and microvoids can trap and condense easily leachable Cs vapour during fabrication. The amorphous triple point regions are sites of accumulation of P and Si. All of these structures contribute to the high first day leach rates in the ceramic, as discussed in detail by Cooper *et al.*, (1986).

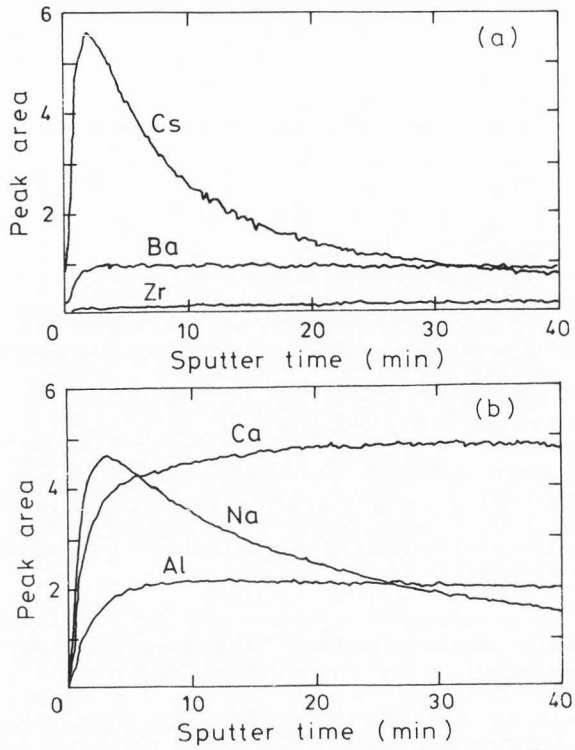

Fig. 9. Static SIMS profiles of a fracture face from a 20wt% HLW-loaded Synroc C disc. SIMS conditions:- 1kV Ar^+; $5x10^{-7}$, $A cm^{-2}$, no charge compensation; 8x8mm, raster, ungated; etch rate ≈ 0.025 nm min^{-1}, i.e. 40 min ≈ 10Å. a. Cs, Ba, Zr; b. Ca, Na, Aℓ.

SAM examination of leached Synroc B (Myhra *et al.*, 1984c) and Synroc C is consistent with the combination of results from the individual phases. Crystallites have been formed after hydrothermal attack with compositions corresponding to TiO_2, ZrO_2, and $CaCO_3$. There is also a mottled background, different from the original unleached Synroc surface, beneath the recrystallised products and covering most of the surface. The fine scale of the material makes resolution of distinct regions difficult but there are areas of predominantly TiO_2, $CaCO_3$, zirconolite, hollandite and Ba/Ti/O (possibly $BaTiO_3$) compositions. It is significant that no areas of $CaTiO_3$ composition were found in the Synroc surfaces leached at high temperature for more than 2 days. Elemental maps of the surface before and after leaching reveal that regions initially rich in Cs, Mo, Ba and Ca are altered to become only weakly differentiated or no longer distinct. These regions are not single phase but, as TEM shows (Cooper *et al.*, 1985), consist of a fine-grained (300nm) mixture with a predominance of one phase (e.g., hollandite, showing a Cs/Ba rich area in a SAM map). The Mo-rich regions are shown, by SAM combined with XPS, to contain O, Ru, Ti and Ag. The surface Mo is in an oxidised form as Mo^{4+} (Myhra *et al.*, 1984c) although the reducing conditions

under which Synroc is made (Reeve *et al.*, 1983) make it likely that this is the result of surface oxidation only.

SEM and TEM characterisation of the effects of leaching on Synroc surfaces has been described in Cooper *et al.*, (1986) and Kastrissios *et al.*, (1987). The initial attack is confined to Mo-rich phases (0.5-1.0 μm in diameter), correlating with the leach rate data and the SAM results. Continued attack produces the same new phases observed by SAM, i.e., those found on the individual minerals. An example of a TEM micrograph in Fig 10 clearly illustrates the loss of surface perovskite grains, the recrystallised TiO_2 products (brookite and anatase) in the perovskite "pores", a low concentration of crystallites on the hollandite phase, and almost no attack on the zirconolite phase. SEM examination of Synroc C leached for 1000 days at 100°C shows that this recrystallised TiO_2 layer continues to grow across the surface but does not form a continuous film. There appears to be very little change in this layer. as observed by SEM, SAM, XPS and SIMS, beyond about 500 days leaching. The leach rates beyond about 100 days become immeasurably small for all elements except Ca, which exhibits considerable variation in rate presumably due to the intersection of the reaction front with new perovskite regions.

This brief selection of data, considered with the more detailed descriptions referenced above, allows us to draw some conclusions about the effect of combining the titanate minerals in the synthetic rock ceramic:-

*the major phases react in the same way as the separate minerals with no obvious synergistic effects on leach rates, leach profiles, surface films or recrystallised products;

*the presence of the microstructural features of intergranular films, pores and triple points introduces new sites for segregation of particular elements in readily-leachable form. This adds to the first day leach rates for these elements but has little effect on leaching beyond a few days;

*the presence of new phases in the ceramic assemblage, particularly those incorporating Mo, produces regions of initially high leachability but, again, their effect on surface reactivity is short-term;

*there is a high degree of consistency between the evidence from the solution analyses, the surface analyses, and the electron microscopy but the interpretation of any one set of results is dependent on understanding of the others.

We will now consider some consequences of the use of these techniques in combination, for the interpretation of leach rates derived from solution analyses.

Congruent and Incongruent Dissolution

The rate of release of a particular element into solution is obviously controlled by the rate of reaction of the solution with the solid, the site of the element in the solid and the formation of new, stable products. We have seen that several types of reaction can occur at titanate surfaces and that, in multiphase ceramics, a particular element can occupy quite different sites in different phases, intergranular films, pores and triple points. Thus, for instance, in Synroc C, Cs is found in hollandite, intergranular films and on pore surfaces; Ca is found in zirconolite, perovskite, magnetoplumbite, intergranular films and triple points. Recrystallised products containing Ti, Zr, Aℓ, Ca and Ba have all been observed on titanate surfaces.

In this context, it is interesting to reexamine the concepts of congruent and incongruent dissolution of minerals and glasses. Dissolution of a separate phase is taken to proceed incongruently if selective cation removal takes place by ion exchange with H_3O^+ from solution while the network or lattice remains intact; this is generally referred to as "leaching", the evidence being primarily derived from very different loss rates for these exchangeable cations as compared with the network forming elements. An ion exchange reaction front is thought to be set up, the direct evidence for which should be altered contrast in TEM micrographs of this region (Clarke, 1981,1982),in advance of any reaction involving disruption of the network or crystalline lattice. XPS, SIMS and SAM depth profiles should show loss of cation concentration to depths considerably greater than those for changes in network element concentrations.

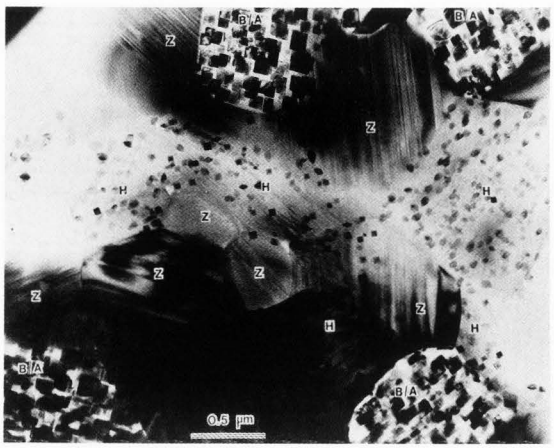

Fig. 10. TEM micrograph of a Synroc B (Ar^+ ion beam-thinned disc) after hydrothermal attack at 190°C for 1 day. Note that the perovskite grains have completely dissolved, recrystallising as brookite (B) and anatase (A) crystals. Hollandite (H) is slightly attacked with a few small TiO_2 crystallites formed. Zirconolite-zirkelite intergrowths (Z) were unaltered by this treatment (Reprinted with permission from Kastrissios *et al.* (1987)).

Congruent dissolution describes a process in which the structure dissolves uniformly. The normalised leach rates for all elements are the same in this case and this is generally referred to as "dissolution" rather than leaching. The reaction front is either at the dissolving surface itself or at the limit of a shallow depletion zone (usually <10nm). Thus, depth profiles and TEM examination should reflect this process, indicating little (or shallow) alteration of the surface.

Both concepts ignore effects of reprecipitation and recrystallisation in nucleated, separate regions of the surface. How realistic, then, are descriptions of leaching and dissolution processes in glasses, minerals and ceramics based on solution analyses alone?

In the case of glasses, incongruent dissolution is found with leach rates differing markedly between the exchangeable cations and the network elements. A pH rise of the water leachant to >10 is another indicator of ion exchange. However, we do not observe altered TEM contrast as H_3O^+ replaces the cations in an intact glass network (Lewis, 1983; Cooper *et al.*, 1986). Instead, the glass network appears to be attacked at the same rate as the ion exchange to form the hydrated, hydrogen bonded (SiOH) siliceous layer observed by IR, SEM and TEM (Hench. *et al.*, 1980; Lewis, 1983). There is no separate ion exchange reaction front observable ahead of a hydrolysed. altered network layer. Of course, the Si in this layer is not released to solution but, equally obviously, it is not unaltered. It appears likely that release of the majority of the cations may require disruption of the glass network. Depth profiles, via XPS, SIMS and SAM, do show concentration gradients of exchangeable cations like Na^+, K^+, Ca^{2+}, Ba^{2+}, Sr^{2+}, etc., but this is consistent with either ion exchange in an intact layer or cation loss from a reacted, hydrolysed layer in which the silicate composition is not significantly altered. XPS, SIMS and IR all give evidence of the formation of SiOH groups in this layer, strongly supporting the latter interpretation. The evidence does not definitely show that glasses are attacked uniformly but the simple view of a cation depletion layer in an intact solid must be questioned. To complicate this description, there is evidence from XPS, SIMS, SEM and TEM of a second reaction zone at the surface in which recrystallisation of reaction products (e.g., β-cristoballite, pyroxenes, orthosilicates, etc.) and segregation of specifically retained elements (e.g., Fe, Mg, Aℓ, Zr) takes place. Incongruency, in this case, does not imply that these elements are retained in their original sites but that they are retained in the reacted surface layer.

Titanate mineral surfaces provide a second case of crystalline materials for comparison with the glasses. The leach rates for perovskite, $CaTiO_3$, clearly indicate incongruent dissolution but all other evidence strongly suggests that congruent dissolution of the whole lattice is the predominant mechanism actually occurring. The SAM, SEM and TEM results tend to show that Ca is not selectively leached from perovskite but that perovskite dissolves, releasing Ca, and recrystallising as anatase and brookite. There is some TEM evidence of a region <20 monolayers deep (i.e.,<8nm) in which the contrast is altered. This could be a narrow region of ion exchange and this is consistent with a pH rise also in this system to pH>10 during reaction under conditions of high surface area to solution volume ratio. The majority of the Ca is released, however, from the reacted titanate layer. The presence of the recrystallised TiO_2 and $CaCO_3$ as isolated crystallites on the surface makes the XPS and SIMS depth profiles difficult to interpret. The observation of substantial Ca loss to 200nm, but Ti and O concentration changes to only 20nm, can now be seen to be consistent with the EM evidence. The important difference between the crystalline (mineral) and glass cases is that, for crystalline titanates, the reacted lattice recrystallises almost immediately and does not leave an amorphous, hydrated layer retaining particular elements.

Similar results and interpretations apply to the other titanate minerals but there is much less reaction (and ion exchange) of hollandite and zirconolite surfaces. This is reflected in the pH changes, to 8-9 with hollandite and to <6 with zirconolite, determined by both ion exchange and $Ti(OH)_x^{n+}$ equilibria (Segall *et al.*, 1985).

The overall dissolution of a multiphase ceramic is likely to be incongruent for the reasons given above, namely different elemental sites and structures, and this is reflected in the leach rates. The contributions from intergranular films, pores, triple points and minor phases has been discussed in Cooper *et al.*, (1985) and (1986). The pH of hydrothermal DDDW solutions containing Synroc C normally stabilises at 4-5 (Levins *et al.*, 1986), indicating less extensive ion exchange than for the separate minerals. Nevertheless, the SAM, SEM and TEM observations strongly suggest that the processes taking place on the grains are the same as those on the separate minerals. The XPS and SIMS depth profiles are particularly difficult to interpret because the perovskite grains in high temperature-reacted samples are usually wholly dissolved to depths of 300-500nm and replaced by TiO_2 crystals. The observed limitation of loss of Ca in these profiles to 200nm is, however, consistent with this. The alteration of Ti and O concentrations in the first 20nm also correctly reflects the presence of discontinuous TiO_2 crystallites on the residual zirconolite/hollandite surface.

In summary, it appears that there are three reaction fronts in both glasses and crystalline titanates after hydrothermal reaction:-

*an ion-exchanged (leached), cation-deficient layer the front of which is no more than 20nm ahead of;

*a reaction layer in which silicate network or titanate lattice breakdown has occurred to give, for glasses, a predominantly amorphous layer and, for titanates, almost complete alteration to new phases;

*a recrystallisation and reprecipitation surface layer in which new, crystalline products are found.

With glasses, the depth of the reaction layer depends on the conditions and duration of attack but can be of the order of mm. The recrystallisation layer can also be >1 μm in depth but most products are in the first 20-100nm. For the minerals, the reaction layer varies from <10nm to about 500nm but appears to be limited to the upper end of this range regardless of reaction conditions and duration. The recrystallised layer can be of the same depth.

Mechanisms of Surface Attack on Titanate Minerals

The kinetics of the dissolution of solids in aqueous solution is now a well-established area of study (Segall *et al.*, 1987). Experience with the dissolution of oxide minerals and oxide glasses provides a reliable basis from which to summarise the major mechanisms contributing to leaching and dissolution of titanate surfaces. They fall into three categories, closely paralleling the description of covalent insulating oxides (Segall *et al.*, 1987) and glasses (Paul, 1982).

Ion exchange reactions

The leaching of alkali metal and alkaline earth cations by ion exchange with H_3O^+ is the mechanism responsible for the loss of the fastest dissolving species, e.g., Cs, Na, Ca, Ba from glasses. The rate is diffusion-controlled initially, as evidenced by a $(time)^{\frac{1}{2}}$ dependence but becomes governed by the slower dissolution of the silicate network,with $(time)^1$ dependence, and eventually by the formation of protective, partially recrystallised surface layers with very low dissolution rate constants and variable time dependence, e.g., Zn with $(time)^0$ dependence (Lewis *et al.*, 1982; Hench *et al.*, 1980). In fact, the leached layer depth becomes the limiting factor in the rate of release of these cations as leaching progresses. In glasses, with their flexible structure (i.e., Si-O-Si bond angles from 120° to 180°), these cations are readily exchanged out of their sites without major structural change to the silicate network. As we have seen, however, the experimental evidence suggests that this process is not more than 20 nm in advance of the process of disruption of the network.

In the crystalline titanates, where these ions are located in lattice positions with much less flexible bond angles, it might be expected that ion exchange, particularly of large cations like Ba^{2+} and Cs^+, would be severely inhibited. The evidence suggests that this is not so; we still see a leached layer <20 monolayers deep (i.e.,<8nm), ahead of the lattice reaction, from which Ca, Ba, Sr have been partially exchanged. This is strikingly evident in room temperature leaching of perovskite powders, where no recrystallisation of TiO_2 is observed. TEM shows that the crystal structure at the surface is intact, but immediate Ca loss corresponding to <5 monolayers is found with an equilibrium loss corresponding to <20 monolayers after 3 days (Pham, unpublished report). There is evidently sufficient flexibility of the lattice to permit this rapid loss. In ceramic assemblages, these cations are also lost very rapidly from amorphous or disordered regions like intergranular films, pores, triple points, etc.

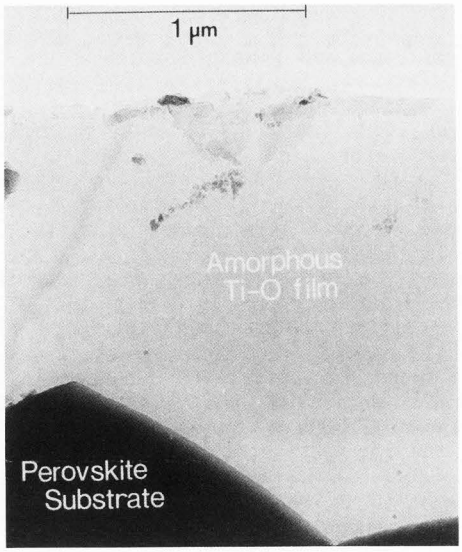

Fig. 11. TEM micrograph of the edge of a pervoskite (Ar^+ ion beam-thinned disc), hydrothermally reacted for 1 day at 110°C, showing an amorphous Ti-O film more than 1 μm wide. (Reprinted with permission from Kastrissios *et al.* (1987)).

We should emphasise that the extent of this ion-exchanged region is relatively very small compared to the depths of reacted layers which can be mm in glasses and of the order of grain sizes in minerals.

Titanate lattice reaction

The base-catalysed hydrolysis of the titanate lattice, corresponding to the reaction producing the siliceous (SiOH) layer in glasses, does not have the same result in titanates. In high temperature hydrothermal attack on titanates, only the recrystallised TiO_2 phases are found. At temperatures below 120°C, we have been able to observe amorphous $Ti-O_x$ films on the edges of ion beam thinned TEM specimens of perovskite, as illustrated in Fig. 11, but there is no evidence that these films contain (TiOH) groups and they are not

found as extensive layers (as they are in glasses) on discs or powder samples. It is clear that they recrystallise to TiO_2, without significant hydration, immediately at temperatures above 120°C and relatively quickly at lower temperatures.

The rate of this reaction varies considerably between the titanate structures. This is also observed with glasses of differing compositions (Lewis, 1983; Hench *et al.*, 1980) where the depth of the siliceous layer can vary from a few hundred Å to mm under the same reaction conditions. In the titanates, this difference in rate is, at least qualitatively, correlated to the structural differences between the minerals (White, *et al.*, 1985). Using coordination of oxygen atoms between TiO_6 octahedra as the entropic factor influencing reaction, we would expect the rate of titanate lattice reaction to be in the order:- perovskites > hollandite > fluorites (e.g., zirconolite) > rutile; this is observed in practice.

The extent of this altered layer is determined by the particular mineral structure, the reaction conditions and the coverage of the surface by TiO_2 product. In Synroc, it is also determined by the grain size which, in turn, is determined by the fabrication conditions and the HLW loading (Cooper *et al.*, 1985). Thus, the size of perovskite grains in Synroc B is generally >1 μm whereas, in Synroc C, it is usually 300nm. More resistant phases underlying the perovskite grains inhibit further attack. The EM observations suggest that only the surface-exposed perovskite grains are lost during hydrothermal attack but the continued detection of Ca in leach analyses up to 1000 days argues that gradual penetration of the material is taking place.

Recrystallisation, reprecipitation and surface segregation

The observations of new phases resulting from reaction have been described for both glass and titanate surfaces. We can distinguish these three cases, however, by considering the combined results from all techniques.

For titanates, the very low concentration of Ti, Zr and Aℓ found in solution at any time after leaching begins, combined with the observation of the metastable Ti-O amorphous films, tends to suggest that the TiO_2, ZrO_2 an $Aℓ_2O_3$ crystallites are formed by recrystallisation on the surface without the majority of the element being released to solution. The evidence is not unequivocal but the presence of TiO_2 crystals deep inside the perovskite "pits", rather than as an overlayer on the surface, argues for *in-situ* recrystallisation. The crystalline products of β-cristoballite and the pyroxenes, formed on Glass #2 (PNL 76-68) are also found within the amorphous siliceous layer and are probably nucleated during network breakdown and diffusion of cationic species in the layer.

Precipitation occurs, for example, in the formation of $CaCO_3$ crystals on titanate surfaces and in the formation of the zinc mineral forms on glass surfaces. The Ca concentration in solution varies systematically with time and pH. It can be correlated with the observation of $CaCO_3$ crystallites on the surface. For instance, no $CaCO_3$ is observed if the Ca concentration is <200 ppm and the pH is held at <6, but precipitates are found at concentration and pH values above this (Pham, unpublished report). They are also characterisically found on the outer surface and not within the surface pits or reacted layer. The crystalline zinc forms occur on the outer surface of glasses suggesting the same reprecipitation mechanism.

There are some elements in depth profiles of glasses that are concentrated in the near-surface region after attack but for which there do not appear to be corresponding crystalline forms. Mg, Fe and sometimes Aℓ are examples. We can speculate that this may be due to incipient crystallisation (kinetically-limited) in which these elements are retained in a stable coordination. with short-range order but no long-range periodicity able to give a diffraction pattern. It is significant that this surface segregation without corresponding crystal forms is not observed on titanate mineral surfaces.

The evidence given in the preceding sections has made clear that the extent of the layer, in which recrystallisation, reprecipitation and segregation occurs, is simply determined by the depth of the lattice (or network) reaction layer. It is important to note that the nature of these processes, involving crystal growth, makes it unlikely that a coherent surface film comprising these reaction products will form in the initial stages of surface modification, although this could occur in long term hydrothermal attack. In the glasses, the often-coherent siliceous layer results from network breakdown, not new crystalline products.

Acknowledgements

The work summarised here includes major contributions from members of the Griffith University Synroc group, particularly Professor Robert Segall, Dr. David Cousens, Dr. Roger Lewis, Dr. Tim White, Theodora Kastrissios, Duy Pham and Mark Stephenson. The assistance of Dr. Des Levins and Mr. Reg Ryan (Australian Nuclear Science and Technology Organization) with leach rate determination, including analyses for data in Table 8, is gratefully acknowledged.

References

Bancroft GM, Brown JR, Fyfe WS. (1979). Advances in, and applications of, Xray photoelectron spectroscopy (ESCA) in mineralogy and geochemistry. Chem.Geol. 25 (3): 227-243.

Buckwalter CQ, Pederson LR. (1983). Inhibition of nuclear waste leaching. Pacific N.W. Labs Report, PNL-SA-9940.

Clark DE, Hench LL. (1981). An overview of the physical characterisation of leached surfaces. Nucl. Chem. Waste Manage. 2: 93-101.

Clarke DR. (1981). Preferential dissolution of an intergranular amorphous phase in a nuclear waste ceramic. J.Amer. Ceram. Soc. 64: 89-90.

Clarke DR. (1982). Application of electron microscopy to the processing of ceramic materials. Ultramicroscopy. 8: 95-108.

Cooper JA, Cousens DR, Lewis RA, Myhra S, Segall RL, Smart RStC, Turner PS, White TJ. (1985). Microstructural characterisation of Synroc C and E by electron microscopy. J.Amer.Ceram.Soc. 68: 64-70.

Cooper JA, Cousens DR, Hanna J, Lewis RA, Myhra S, Segall RL, Smart RStC, Turner PS, White TJ. (1986). Intergranular films and pore surfaces in Synroc C: structure, composition and dissolution characteristics. J.Amer.Ceram.Soc. 69: 347-352.

Cousens DR, Lewis RA, Myhra S, Segall RL, Smart RStC, Turner PS. (1982a). Evaluating glasses for high level radioactive waste immobilisation - a review. Radioact. Waste Manage. 2: 143-168.

Cousens DR, Lewis RA, Myhra S, Segall RL, Smart RStC, Turner PS. (1982b). The chemical durability of some HLW glasses: effects of hydrothermal conditions and ionising radiation, in Scientific Basis for Nuclear Waste Management, Vol 5 (North Holland. Amsterd.) pp 163-171.

Dillard JG, Koppelman MH. (1975). XPS in the study of mineral materials. Eos (Am. Geophys. Union Trans.) 56: 12.

Dosch RG, Lynch AW. (1980). Solution chemistry techniques in Synroc preparation. Sandia Lab Report SAND 80-2375.

Dosch RG, Headley TJ, North CJ, Hlava PF. (1983). Processing, microstructure, leaching and long term stability studies related to titanate high level waste forms. Sandia Lab. Report SAND-82-2980.

Farmer VC. (1974). The lnfrared Spectra of Minerals. Mineralog Soc. London pp.285-303.

Freeborn WP, White WB. (1984). Hydrothermal dissolution of nuclear waste ceramics. in Nuclear Waste Ceramics (Eds) GG. Wicks, WA. Ross, Amer. Ceram. Soc., Columbus, Ohio. pp 368-376.

Hench LL, Clark DE and Lue Yen-Bower E. (1980). Surface leaching of glass and glass-ceramics. Nucl.Chem.Waste Manage. 59: 1-39

Hollister CD, Anderson DR, Heath GR. (1981). Seabed disposal of nuclear wastes. Science 213: 1321-1326.

Jacquet-Francillon N, Pacaud F, Queille P. (1982) in Scientific Basis for Nuclear Waste Management, Vol. 5, Materials Research Soc. Proc., Plenum Press, N.Y : 249.

Jantzen CM, Clarke DR, Morgan PED, Harker AD.(1982). Leaching of polyphase nuclear waste ceramics: microstructural and phase characterisation. J.Amer.Ceram.Soc. 65: 292-300.

Kastrissios T, Stephenson M, Turner PS, White TJ. (1987). Hydrothermal dissolution of perovskite:- implications for Synroc formulation. J Amer. Ceram.Soc.70: C144-146.

Kesson SE. (1983). The immobilisation of cesium in Synroc hollandite. Radioact.Waste Manage. 4: 53-72.

Kesson SE, Sinclair WJ, Ringwood AE. (1983). Solid solution limits in Synroc zirconolite. Nucl.Chem.Waste Manage. 4: 259-265.

Koppelman MH. (1980). Application of XPS to the study of mineral surface chemistry, in Advanced Chemical Methods for Soil and Clay Minerals Research, NATO Adv.Study Ser., Ser.C., 63: 205-240.

Levins DM, Reeve KD, Buykx WJ, Ryan RK, Seatonberry BW, Woolfrey JL. (1986). Fabrication and performance of Synroc. in Spectrum '86, Proc. ANS Int. Topical Meeting on Waste Management, Decontamination and Decommissioning, in press.

Lewis RA, Myhra S, Segall RL, Smart RStC, Turner PS. (1982). The surface layer formed on zinc-containing glass during aqueous attack. J.Non-Cryst.Solids 53: 299-313.

Lewis RA. (1983). Hydrothermal dissolution of nuclear waste glasses. Thesis, Griffith University, Brisbane, Australia, pp 1-192.

Malm DL, Vasile FJ, Padden GJ, Dove DB, Pantano Jr. CG. (1978). Depth profiles of Na and Ca in glasses: a comparison of SIMS and Auger analysis. J.Vac.Sci.Technol. 15: 35.

McCarthy GJ, White WB, Roy R, Scheetz BE, Komarneni S, Smith DK, Roy DM. (1978). Interactions between nuclear waste and surrounding rock. Nature 273: 216.

McCarthy GJ, Scheetz BE, Komarneni S, Smith DK, White WB. (1980). Hydrothermal stability of simulated radioactive waste glass, in Solid State Chemistry: A Contemporary Overview. Advances in Chemistry Series #186. (Eds) SL. Holt, JB. Milstein, M Robbins. Amer.Ceram.Soc., Columbia, Ohio.

McIntyre NS, Strathdee GC, Phillips BF. (1980). SIMS studies of the aqueous leaching of a borosilicate glass. Surf. Sci. 100: 71.

McVay GL, Pederson LR. (1981). Effect of γ irradiation on glass leaching. J. Amer. Ceram.Soc 64: 154-8.

McVay GL, Buckwalter CQ. (1984). The effect of iron on waste glass leaching Pacific N.W. Labs Report. PNL-SA-10474.

Mendel JE. (1982). The measurement of leach rates: a review. Nucl. Chem.Waste Manage. 3: 117-123.

Mendel JE. (1983). One year leach test data for PNL 76-68 (Batch 4) glass. in Materials Characterisation Center Test Methods. MCC-D1, Pacific N.W. Labs Report, PNL 3996.

Metson JB, Bancroft GM, Kanetkar SM, Nesbitt HW, Fyfe WS.(1982) in Scientific Basis for Nuclear Waste Management Vol. 5, Mat.Res. Soc. Symp. Proc., Plenum. N.Y., 329.

Morgan PED, Clarke DR, Jantzen CM, Harker AB, (1981). High-alumina tailored nuclear waste ceramics. J. Amer.Ceram.Soc. 64: 249-258.

Myhra S, Bishop HE, Riviere JC. (1983a). Investigation by XPS of surface features of some titanate minerals. Surface Tech. 19: 161-172.

Myhra S, Bishop HE, Riviere JC. (1983b). Surface analytical features of Synroc B and C. Surface Tech. 19: 145-160.

Myhra S, Segall RL, Smart RStC, Turner PS, (1984a). The adequacy of glass as a solid for high level radioactive waste disposal: a public perspective. Atomic Energy in Australia 27: 42-47.

Myhra S, Savage D, Atkinson A, Riviere JC. (1984b). Surface modification of some titanate minerals subjected to hydrothermal chemical attack. Amer. Mineral. 89: 902-909.

Myhra S, Atkinson A, Riviere JC, Savage D. (1984c). A surface analytical study of Synroc subjected to hydrothermal attack. J.Amer.Ceram Soc. 67: 223-227.

Myhra S, Bishop HE, Riviere JC, Stephenson M. (1987). The hydrothermal dissolution of perovskite ($CaTiO_3$). J. Mat. Sci. 22: 3217-3227.

Nesbitt HW, Bancroft GM, Fyfe WS, Karkhanis SN, Nishijima A, Shin S. (1981). Thermodynamic stability and kinetics of perovskite dissolution. Nature 289: 358-362.

Oversby VM, Ringwood AE. (1982). Leaching studies on Synroc C at 95°C and 200°C. Radioact.Waste Manage. 2: 223-227.

Paul A. (1982). The Chemistry of Glasses. Chapman and Hall, London.

Reeve KD, Levins DM, Ramm EJ, Woolfrey JL. (1983). The development and evaluation of Synroc for high level radioactive waste immobilisation. Proc.Int. Symp. Cond. Radioactive Waste for Storage and Disposal. IAEA-SM-261 (Vienna) pp 375-402.

Ringwood AE. (1978). Safe Disposal of High Level Nuclear Reactor Waste: A New Strategy. ANU Press, Canberra.

Ringwood AE, Oversby VM, Kesson SE, Sinclair W, Ware N, Hibberson W, Major A. (1981). Immobilisation of high level nuclear reactor wastes in Synroc: a current appraisal.Nucl. Chem.Waste Manage. 2; 287-305.

Rusin JM, Lokken RO, May RP, Wald JW. (1982). Crystallization behavior of nuclear waste forms. In Proc. Symp.High Temp.Material Chemistry, (Eds) Cubicciotti DD and Hildenbrand DL. Electrochem Soc., N.Y. p.133.

Savage D, Chapman NA. (1982). Hydrothermal behaviour of simulated waste glass and waste rock interactions under repository conditions, in Geochemistry of Radioactive Waste Disposal (Eds) GW. Bird, WS. Fyfe, Chem.Geol. 36: 59-86.

Segall RL, Myhra S, Smart RStC, Turner PS. (1985). Evaluation of critical properties of Synroc for disposal of high level radioactive waste. Final Report NERDDC Project No. 80/0049, Aust. Govt.Publishing Office pp 1-186.

Segall RL, Smart RStC, Turner PS. (1987). Oxide surfaces in solution. in Surface Chemistry of Oxide Materials (Eds) L-C. Dufour and J. Nowotny (Elsevier, Amsterdam),in press.

Scheetz BE, White WB, Atkinson SA. (1982) Dissolution of Aℓ-, Ti- and Zr-based crystalline waste form components under hydrothermal conditions. Nucl.Tech. 56: 289-296.

Sill CW. (1982). Some deficiencies in analysing leachates and reporting results. Nucl. Chem. Waste Manage. 3: 141-147.

Smart RStC. (1985). The validity of SIMS observations of alkali metal segregation into intergranular regions of ceramics. Appl. Surface Sci. 22/23; 90-99.

White TJ, Segall RL, Turner PS. (1985). Radwaste immobilisation by structural modification - the crystallochemical properties of Synroc, a titanate ceramic. Angew.Chemie (Int.Ed.Engl.) 24:357-365.

White TJ, Fielding PE. (1987). Crystal chemical incorporation of high level waste species in alumino titanate - based ceramics: valence, location, radiation damage and hydrothermal durability. J. Mat. Res., in press

Wolery TJ. (1979). Calculations of chemical equilibrium between aqueous solution and minerals: the EQ3/6 software package. Lawrence Livermore Labs Report UCRL 52658.

Discussions with Reviewers

G. Remond: As pointed out by the authors, the reliability of data obtained with surface sensitive techniques depends upon the specimen preparation procedure used. The preparation technique may also induce surface composition changes. Could the reactivity rate of the material in a leaching experimentation be affected by the initial surface composition resulting from specimen preparation i.e. is a surface attack behaviour identical for the same specimen being ground, fractured or polished?

R. Gijbels: The authors state that results can be influenced by sample preparation, e.g. cutting and polishing discs in water.. It is conceivable that even dry cutting and polishing will already introduce mechanical stress in the surface, which will influence subsequent dissolution behaviour. Could the authors comment on this?

Authors: There are distinct differences in surface reactivity and composition profiles induced by surface preparation. For instance, cutting or polishing any of these materials in water causes loss of alkali metal cations and, in some cases, Ca^{2+}, Mg^{2+}, Sr^{2+}, Ba^{2+} from the near-surface region before any leaching experiments are carried out. It is essential to prepare the surfaces under dry alcohol or similar non-leaching solvents. Fracture faces on all ceramics and minerals tend to expose intergranular regions usually containing segregated elements in higher concentration than the bulk composition e.g. Cs, Na, Si, Aℓ, P. In multiphase ceramics and rocks, these intergranular regions are amorphous and can be from 20Å to 10μm wide. These segregated elements are often lost immediately on exposure to solution, giving higher initial loss rates when compared with polished surfaces. For this reason, ground powders of minerals and ceramics can give different leach rates (per unit surface area) than polished discs. Glasses do not exhibit this complication.

There is a continuing controversy on the extent of damage (if any) introduced to the

surface layers by such operations as cutting, grinding and polishing. Using high resolution transmission electron microscopy, we have not been able to observe any disordered layer or extensive strain contrast due to grinding or polishing, although dislocations in grains and incipient fracture at intergranular boundaries is often observed. With ground particles of pure minerals like perovskite, the lattice fringes, indicating crystal periodicity, continue to within a few Å of the surface.

R. Gijbels: Could the authors make some comments on the existing controversy in the mineralogical/geological literature concerning congruent/incongruent dissolution of silicate minerals, e.g. feldspars, plagioclases, pyroxenes, amphiboles? This could help in making the bridge between silicate glasses and titanate minerals.

Authors: The first and most important comment is that the evidence from surface techniques and electron microscopy, of the type discussed in our review, has clearly shown that inferences of congruent or incongruent dissolution based on solution analyses and dissolution kinetics alone can be seriously misleading. In many examples of mineral, ceramic and glass surfaces, recrystallisation to new crystal forms takes place *in situ* without loss of the elements to solution. The new crystallites can be very small (i.e. 1-100 nm) and difficult to image or analyse. Additionally, surface layers and amorphous, surface-segregated regions with metastable (possibly incipiently crystalline) reaction products resulting from lattice attack, can be found.

A diagram kindly supplied by the reviewer (R. Gijbels) summarised these processes. Our review makes clear that not all of these processes necessarily occur in a particular case. The depths of the different layers can also vary substantially, between minerals, ceramics and glasses.

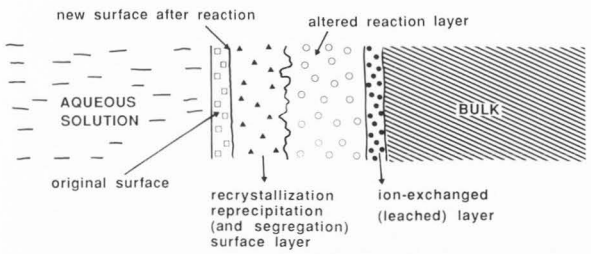

With this in mind, we believe that a description of the dissolution process as "congruent" or "incongruent" is not adequate or useful. The more important questions are, in essence: (i) "Is the release of elements from the lattice due to ion exchange without lattice distortion or is hydrolysis of the lattice necessary before the ions can move?" and (ii) "Does the element dissolve in solution, recrystallise to a new phase *in situ*, or segregate into an amorphous surface layer?" For solution conditions approaching saturation limits, there is also the possibility of reprecipitation but this can be avoided in practice. Evidence to answer these questions requires some very detailed examination of the altered surface layers. We cannot yet claim to have fully articulated these mechanisms for the titanate minerals.

Applying these considerations to the dissolution of silicate minerals, it is our view that the current discussion, summarised for instance for feldspar dissolution in the paper by Chou L, Wollast R, (1984) - Study of the weathering of albite at room temperature and pressure with a fluidized bed reactor. Geochim. Cosmochim. Acta. 48: 2205-2217, can only be resolved by combining the dissolution kinetics models (e.g. Aagaard P, Helgeson HC (1982) - Thermodynamic and kinetic constraints on reaction rates among minerals and aqueous solutions. I Theoretical considerations. Amer. J. Sci. 282: 237-285) with evidence from surface analysis and electron microscopy. Thus, Chou and Wollast (1984) referenced above, suggest that Na is lost from the first few tens of Angstroms of albite after 1 day at 100°C in DDDW but Rutherford backscattering and resonant nuclear reaction data (Petit JC, Dran JC, Schott J, Della Mea G (1986) - New evidence on the dissolution mechanism of crystalline silicates by ion beam techniques. 5th Int. Symp. Water Rock Interaction, Reykjavik, Iceland, August, 1986, extended abstract) show penetration of hydrogen to depths in excess of 500Å. Our SIMS data on hydrothermal attack of perovskite give TiOH and CaOH species to depths greater than 300Å even after low temperature (<100°C) attack. XPS on the same samples, however, does not show Ca loss at the surface. It may be that the silicate (and titanate) lattices are hydrolysing, possibly at local sites like intergranular regions and defects, and that loss of Na (or Ca) to solution is dependent on the reaction but is relatively slow.

We are currently attempting to define this process more clearly with evidence from single grains, integranular regions and polycrystalline discs of titanate minerals. We expect from the experience with silicate glasses that the methods and mechanisms will be equally applicable to silicate minerals.

R. Gijbels: It appears that experimental weathering data on silicate minerals can more easily be interpreted in suitable experimental conditions, such as for powdered samples in a fluidized bed reactor (see paper by Chou and Wollast), e.g. by staying more easily below the solubility product of secondary minerals such as AlOOH etc. Although this approach may not be relevant in nuclear waste disposal, it would be useful to have the authors' comments on what they expect to happen in such conditions with titanate minerals.

Authors: We have examined data for both titanate minerals and silicate glasses over a very wide range of under-saturation and over-saturation conditions by varying the solution volume/surface area ratio. The sophisticated program and data base EQ3/6, developed by Wolery (1979) (text reference)

with our additions for Ti phases, predicts equilibria between aqueous solution andprecipitated mineral phases as well as the kinetics of their formation. In practice, we observe several such phases as for instance calcite, boehmite, gibbsite, $BaMoO_4$, $BaSO_4$ at over-saturation conditions. Equally importantly, however, we do not observe other predicted phases, eg. sphene, kaolin, smectite clays, and we do observe some new minerals at under-saturation, e.g. anatase, brookite, calcite, zirconia suggesting that local compositions, pH, etc. in the hydrolysed surface layers of the solid and solution electrical double layer may be considerably different from bulk solution conditions.

With titanate minerals, as with silicate minerals, it is certainly easier to interpret results from initial dissolution using large solution volume/surface area ratios.

R. Gijbels: An interesting aspect of including surface analytical techniques in water-rock interaction studies is the direct confirmation of H-incorporation into the altered surface layer. For silicate glasses this has been done, e.g. by IR spectroscopy (SiOH vibration frequency), but for minerals there appears to be almost no information. Would it be possible to detect any incorporation of hydrogen in reacted perovskite surface (TiOH), for instance, by more sensitive techniques such as SIMS or charged particle induced nuclear reactions? (Petit *et al*, 1986, reference above).

Authors: We have mentioned above that SIMS does indeed detect some TiOH and CaOH in reacted perovskite surfaces to depths of 300-500Å. IR spectroscopy in the ATR mode does not detect ν(OH) vibrations because this layer forms only a small proportion of the ~0.5μm layer sampled by the IR beam.

There remain unexplained differences between results from electron microscopy, which show unaltered powder grains, and from surface analyses, which show OH species in depth profiles of discs, for perovskite leached at room temperature. Defects and intergranular regions may be responsible for these differences but more direct evidence is required before this can be clarified